Book Chapter

Voltage and Time Required for Irreversible Thermal Damage of Tumor Tissues during Electrochemotherapy under Thomson Effect

Hamdy M Youssef[1,2]* and Alaa A El-Bary[3]

[1]Mathematics Department, Faculty of Education, Alexandria University, Egypt
[2]Mechanical Engineering Department, College of Engineering and Islamic Architecture, Umm Al-Qura University, KSA
[3]Basic and Applied Science Institute, Arab Academy for Science, Technology, and Maritime Transport, Egypt

***Corresponding Author:** Hamdy M Youssef, Mechanical Engineering Department, College of Engineering and Islamic Architecture, Umm Al-Qura University, Makkah, KSA

Published **March 17, 2021**

This Book Chapter is a republication of an article published by Hamdy M Youssef and Alaa A El-Bary at Mathematics in September 2020. (Youssef, H.M.; El-Bary, A.A. Voltage and Time Required for Irreversible Thermal Damage of Tumor Tissues during Electrochemotherapy under Thomson Effect. Mathematics 2020, 8, 1488. https://doi.org/10.3390/math8091488)

How to cite this book chapter: Hamdy M Youssef, Alaa A El-Bary. Voltage and Time Required for Irreversible Thermal Damage of Tumor Tissues during Electrochemotherapy under Thomson Effect. In: Leonid Shaikhet, editor. Prime Archives in Applied Mathematics: 2nd Edition. Hyderabad, India: Vide Leaf. 2021.

Author Contributions: Conceptualization, H.Y. and A.E.; methodology, H.Y., and A.E.; formal analysis, H.Y; investigation, A.E.; resources, H.Y. and A.E.; writing—original draft preparation, H.Y., and A.E.; writing—review and editing, A.E.; visualization, H.Y.; supervision.

Funding: This research received no external funding.

Acknowledgments: The authors are grateful for the support of this work as a part of the project provided by the "Long-Term Comprehensive National Plan for Science, Technology, and Innovation" through STU of Umm Al-Qura University.

Funding: This work was supported by the Long-Term Comprehensive National Plan for Science, Technology, and Innovation [Grant numbers: 14-MAT162-10 with amount 500,000.00 SR]. H. Youssef is the P-I of the project, and N. Alghamdi is the Co-I of the project.

Conflicts of Interest: The authors declare no conflict of interest.

Abstract

The essential target of the tumor's treatment is how to destroy its tissues. This work is dealing with the thermal damage of the tumor tissue due to the thermoelectrical effect based on the Thomson effect. The governing equation of tumor tissue in concentric spherical space based on the thermal lagging effect is constructed and solved when the surface of the tumor tissue is subjected to a specific electric voltage. Different voltages and resistances effects have been studied and discussed for three different types of tumor tissues. The thermal damage quantity has been calculated with varying values of voltages and times. The voltage has significant effects on the temperature and the

amount of irreversible thermal damage to the tumor. Electrotherapy is a successful treatment. This work introduces a different model to doctors who work in clinical cancer to do experiments about using electricity to damage the cancer cells.

Keywords

Electrotherapy; Thermal Lagging; Thermal Damage; Tumor tissue; Thomson Effect

Introduction

Electrochemotherapy with a low-level direct electric current (DEC) is a therapeutic approach that consists of applying a direct current electric across the tumor tissues, and it has been proved to be a sure, effective, and relatively cheap treatment of tumors [1]. Currently, electrochemotherapy procedure has been performed in several cancer clinics based on standardized clinical protocol [2]. The electrical properties of living tissues have been studied by many researchers to evaluate the effect of electromagnetic fields [3]. Nuccitelli discussed the use of pulsed electric fields in cancer therapy based on pulse length, millisecond domain, microsecond domain, and nanosecond domain [4]. Gabriel et al. introduced one of the most essential and complete data on the electrical properties of tissues in the full range of $10\text{Hz} - 20\,\text{GHz}$ [5]. Many authors have confirmed that the electrical properties of all types of tumor tissue (muscle, fat, breast, etc.) vary after applying electroporation pulses [5-11]. Tasi et al. have determined the in-vivo dielectric properties, resistivity, and relative permittivity of living epidermis and dermis of human skin soaked with a physiological saline solution for one minute between 1 kHz and 1 MHz [12].

We have three common types of tumors. The first type is called a lipoma tumor, which is a fatty tissue tumor. The second type is the liposarcoma tumor that arises in deep and fat cells of the soft tissue. The third type is called myxoid liposarcoma tumor, which is characterized by round to oval cells. The resistance values of the above three types of tumors have been calculated. The

myxoid liposarcoma tumors show resistance values (50 Ω -100 Ω). The liposarcoma tumors show resistance values (250 Ω -970 Ω), while lipoma tumors show resistance (800 Ω -1800 Ω) [13].

The dual-phase-lag (DPL) model is a heat conduction model that describes the temperature on a macroscopic scale with the microstructural effect by taking into account the phase-lag-times of temperature gradient and heat flux [14,15]. It has been applied to studying various problems of heat transfer. Many authors investigated the effects of the phase lag times of heat flux and temperature gradient on the thermal wave transfer inside the tissues [16-29]. Mathematical modeling is essential for scientific studies, and industrial and is widely used in treatment planning [30]. Nuccitelli solved an application of Pulsed Electric Fields to cancer therapy, where he found that nanosecond pulsed fields to be effective in treating skin lesions but have not yet been approved for cancer therapy [4]. Calzado et al. constructed Simulations of the electrostatic field, temperature, and tissue damage generated by multiple electrodes for electrochemical treatment [31]. Soba et al. have integrated the analysis of the potential, electric field, temperature, P.H., and tissue damage, which has been generated by different electrode arrays in a tumor under electrochemical treatment [32]. Aguilera et al. studied the electric current density distribution in planar solid tumor and its surrounding healthy tissue generated by an electrode elliptic array used in electrotherapy [33]. Luo et al. studied the tumor treating fields for high-grade gliomas [34].

Any electrical conductor has two different thermoelectric effects, the Peltier and Thomson effects, which are responsible for the thermal dissipation. Those effects are going in a conductor material when the electrical current passes through it. Within the Thomson effect, the absorption of heat occurs when the electric current goes through a circuit composed of a single material that has a gradient of temperature along its length. The Thomson effect is considered as a heat source/sink, commonly, which is added to the Joule-heating. Some attempted has to consider the Thomson effect, but only for a specific case [35]. Chen et al. studied a model in which the Thomson effect and determined a

threshold criterion for neglecting the Thomson effect based on material properties [36].

No data for the value of the Thomson effect coefficient (Seebeck coefficient) has been found for the skin tissue or to the tumor as an electrical conductor material. So, the values of that coefficient have been assumed to study the effect of this phenomenon on tumors.

Goodarzi et al. develop the lattice Boltzmann method to simulate the slip velocity and temperature domain of buoyancy forces of FMWCNT nanoparticles in water through a microflow imposed to the specified heat flux and constructed the numerical simulation of natural convection heat transfer of nanofluid with nanoparticles in a cavity with different aspect ratios [37-39].

The DPL bioheat conduction model could significantly predict the different temperatures and thermal damage in any tissues from the hyperbolic equation of thermal wave and Fourier's heat conduction models. Moreover, the DPL bioheat conduction equations can be reduced to the Fourier heat conduction equations only if both phase lag times of the temperature gradient and the heat flux is zero *[40]*.

This work is a theoretical investigation for the thermoelectrical effect on three different types of tumor tissues that have different known values of resistance. This study does not discuss the impact of the phase-lag parameters, which already has been done in many publications. The aim is to know the values of the suitable electric voltage and time required to do enough irreversible thermal damage for the three different types of tumors.

Materials and Methods

A small volume of tumor is considered as a solid sphere with the radius R [41]. Cancer occupies the region $0 \le r \le R$, and the temperature distributes over it with a function of the distance r from the center of the sphere and time t (see Figure 1).

We consider three different types of tumors with the same histological features; myxoid liposarcoma, liposarcoma, and lipoma.

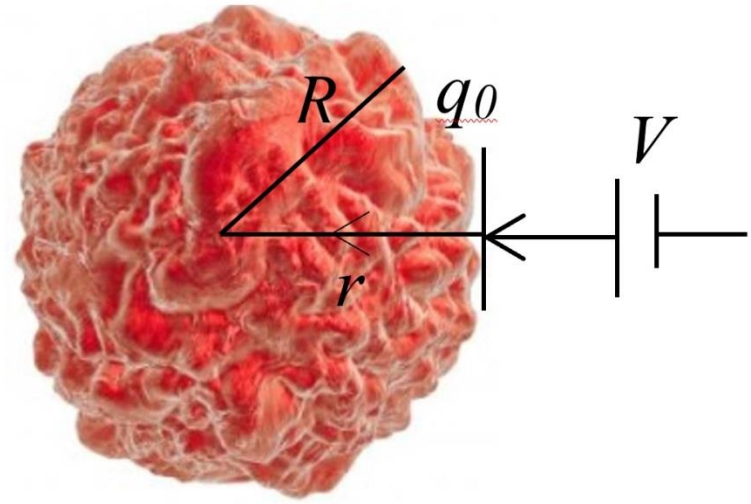

Figure 1: A tumor is subjected to a thermoelectrical source with voltage *V*

The heat conduction equation takes the form [15,21,28,29,41]:

$$K\nabla T\left(r,t+\tau_T\right)=-q\left(r,t+\tau_q\right) \tag{1}$$

where $T=T\left(r,t\right)$ is the effective temperature, *K* is the thermal conductivity, $q=q\left(r,t\right)$ is the heat flux, *t* is the time, and τ_q,τ_T are the phase-lag-time parameters of the heat flux and the temperature gradient, respectively.

In general, the relaxation times τ_q,τ_T are minimal, and we maybe neglect them, but in the biological and living materials, those parameters are very significant.

The energy conservation formula of bioheat transfer is given by [15,21,28,29,41,42]:

$$\rho C\frac{\partial T}{\partial t}=-\nabla\cdot q-w_bC_b\rho_b\left(T-T_0\right)+\left(q_m+q_{ext}\right) \tag{2}$$

The term $w_bC_b\left(T-T_0\right)$ is the heat due to convection into the tumor per unit mass, and it is homogenous, ρ_b, C_b and w_b are the density, specific heat, and perfusion rate of blood, respectively. q_m is the metabolic heat generation, q_{ext} is the external heat source, and $T_0=37\,^oC$ is the reference temperature of the tumor.

The first-order Taylor series of the DPL model can be written as:

$$K\left(1+\tau_T\frac{\partial}{\partial t}\right)\nabla T=-\left(1+\tau_q\frac{\partial}{\partial t}\right)q \tag{3}$$

which gives

$$K\left(1+\tau_T\frac{\partial}{\partial t}\right)\nabla^2T=-\left(1+\tau_q\frac{\partial}{\partial t}\right)\nabla\cdot q \tag{4}$$

Almost all the tumor types take a spherical shape with different sizes, so we assumed the body of our application is a spherical body.

The differential equation of bio-heat transfer in the spherical coordinate system is obtained from equations (2) and (4) as:

$$K\left(1+\tau_T\frac{\partial}{\partial t}\right)\frac{1}{r^2}\frac{\partial}{\partial r}\left(r^2\frac{\partial T}{\partial r}\right)=\left(1+\tau_q\frac{\partial}{\partial t}\right)\left(\rho C\frac{\partial T}{\partial t}+w_b\rho_bC_b\left(T-T_0\right)-q_m-q_{ext}\right) \tag{5}$$

Consider the following functions [41]:

$$\left(T - T_0\right) = \frac{\theta}{r} \tag{6}$$

Thus, we have

$$\nabla^2 T = \frac{1}{r^2}\frac{\partial}{\partial r}\left(r^2 \frac{\partial T}{\partial r}\right) = \frac{1}{r}\frac{\partial^2 \theta}{\partial r^2} \tag{7}$$

Hence, we have from equations (5)-(7) that:

$$K\left(1+\tau_T \frac{\partial}{\partial t}\right)\frac{\partial^2 \theta}{\partial r^2} = \left(1+\tau_q \frac{\partial}{\partial t}\right)\left(\rho C \frac{\partial \theta}{\partial t} + w_b \rho_b C_b \theta\left(r,t\right) - r q_m - r q_{ext}\right) \tag{8}$$

Consider that the tumor is working as a conductor with electrical resistance $R_e\left(\Omega\right)$, and the surface of the tumor $r = R$ is subjected to a particular heating source that comes from the thermal effect due to connection with electric voltage *V(V)* and current *I(A)*. Then, the heat flux is given by:

$$q_{ext} = \frac{V^2}{R_e}t + \alpha I \nabla T = \frac{V^2}{R_e}t + \alpha \frac{V}{R_e}\frac{\partial T}{\partial r} \tag{9}$$

where α is the Seebeck coefficient.

The Seebeck coefficient (also known as thermoelectric power, thermopower, and thermoelectric sensitivity) of a material is a measure of the magnitude of an induced thermoelectric voltage in response to a temperature difference across that material.

$$q_{ext} = \frac{V^2}{R_e}t + \frac{\alpha V}{R_e}\left[\frac{1}{r}\frac{\partial \theta}{\partial r} - \frac{\theta}{r^2}\right] \tag{10}$$

Applying Laplace transform for equation (8) and (9) defined as:

$$\overline{f}(s)=\int_0^{\infty} f(t)e^{-st}dt \tag{11}$$

Then, we have

$$\overline{q}_{ext}=\frac{V^2}{R_e s^2}+\frac{\alpha V}{R_e}\left[\frac{1}{r}\frac{\partial\overline{\theta}}{\partial r}-\frac{\overline{\theta}}{r^2}\right] \tag{12}$$

The following initial conditions have been used within applying the Laplace transform:

$$\theta(r,t)\Big|_{t=0}=0 \text{ and } \frac{\partial\theta(r,t)}{\partial t}\Big|_{t=0}=0 \tag{13}$$

Thus, we get

$$\frac{d^2\overline{\theta}}{dr^2}+\frac{\alpha Vh}{R_e}\frac{d\overline{\theta}}{dr}-h\left(\rho C s+w_b\rho_b C_b+\frac{\alpha V}{rR_e}\right)\overline{\theta}=-rh\left(\overline{q}_m+\frac{V^2}{R_e s^2}\right) \tag{14}$$

where $h=\frac{(1+\tau_q s)}{K(1+\tau_T s)}$, $\overline{q}_m=\frac{q_m}{s}$, and $\frac{\alpha Vh}{rR_e}\Big|_{r\approx R/2}\approx\frac{2\alpha Vh}{RR_e}$

(This term has a small value in the tissue applications. Thus, we can use a linear form without loss of generality).
Hence, we have

$$\frac{d^2\overline{\theta}}{dr^2}+l\frac{d\overline{\theta}}{dr}-m\overline{\theta}=-nr \tag{15}$$

where $l=\frac{\alpha Vh}{R_e}$, $m=h\left(\rho C s+w_b\rho_b C_b+\frac{2\alpha V}{RR_e}\right)$,

$n=h\left(\overline{q}_m+\frac{V^2}{R_e s^2}\right)$

The general solution of equation (15) takes the form

$$\bar{\theta}(r,s) = c_1 e^{k_1 r} + c_2 e^{k_2 r} + \frac{n}{m} r + \frac{nl}{m^2} \tag{16}$$

where k_1, k_2 are the roots of the characteristic equation:

$$k^2 + l\,k - m = 0 \tag{17}$$

Apply the following boundary conditions:

$$\theta(r,t)\big|_{r=0} = 0, \qquad \nabla T(r,t) = \frac{1}{r}\frac{\partial \theta(r,t)}{\partial r} - \frac{\theta(r,t)}{r^2}\bigg|_{r=R} = -\frac{q_0}{K}$$

where $q_0 = \frac{V^2}{R_e} t$ is the applied external heat flux due to the electric voltage *V* and negative value because it goes towards the origin in a negative direction.

Using Laplace transform defined in (11), we get:

$$\bar{\theta}(r,s)\big|_{r=0} = 0, \qquad \frac{1}{r}\frac{\partial \bar{\theta}(r,s)}{\partial r} - \frac{\bar{\theta}(r,s)}{r^2}\bigg|_{r=R} = \frac{\bar{q}_0}{K} \tag{19}$$

where $\bar{q}_0 = \frac{V^2}{R_e s^2}$.

Thus, we have the following system of linear equations:

$$c_1 + c_2 = -\frac{nl}{m^2} \tag{20}$$

$$\left(k_1 R - 1\right) e^{k_1 R} c_1 + \left(k_2 R - 1\right) e^{k_2 R} c_2 = \frac{R^2 \bar{q}_0}{K} + \frac{nl}{m^2} \tag{21}$$

Solving the above system gives the following equation:

$$\bar{\theta}(r,s)=\frac{1}{(k_1R+1)e^{k_1R}-(k_2R+1)e^{k_2R}}\left[\begin{array}{l}\left(\frac{nl}{m^2}(k_2R+1)e^{k_2R}+\frac{nl}{m^2}+\frac{R^2\bar{q}_0}{K}\right)e^{k_1r}-\\ \left(\frac{nl}{m^2}(k_1R+1)e^{k_1R}+\frac{nl}{m^2}+\frac{R^2\bar{q}_0}{K}\right)e^{k_2r}\end{array}\right]+\frac{n}{m}r+\frac{nl}{m^2} \tag{22}$$

which is the final solution in the Laplace transform domain.

The Thermal Damage

Henriques and Moritz used the Arrhenius formula to calculate the thermal damage [43]. They proposed that the thermal damage of the tissue could be considered as a chemical rate process, and calculated by using the first-order Arrhenius rate equation. The measure of thermal damage ω was introduced, and its rate $\kappa(T)$ was supposed to satisfy [43-45]:

$$\frac{d\omega}{dt}=\kappa(T)=A\exp\left(-\frac{E_a/\eta}{T}\right) \tag{23}$$

which gives

$$\omega=A\int_0^t\exp\left(-\frac{E_a/\eta}{T}\right)dt \tag{24}$$

where A is a frequency factor, η is the universal gas constant, and E_a is the activation energy.

Equation (23) explains that a reaction proceeds go faster with larger values of T or A for the same E_a, or with a smaller value of E_a for the equal value of A. So, the parameters A and E_a are usually obtained experimentally.

The reaction rate of the thermal damage process is given as [46]:

$$\kappa(T)=\exp\left[(E_a-21149.32)/2688.37\right]\exp\left(-\frac{E_a/\eta}{T}\right),\ T\geq 55\,^oC \tag{25}$$

Hence, we obtain the thermal damage in the form:

$$\omega=\exp\left[(E_a-21149.32)/2688.37\right]\int_0^t\exp\left(-\frac{E_a/\eta}{T(t)}\right)dt,\ T\geq 55\,^oC \tag{26}$$

Arrhenius assumed that $\omega=1.0$ denotes the beginning of irreversible damage and $\omega<1.0$ denotes the reversible damage [43-46].

There are differences between the coefficients used in the burn damage integral due to the different experimental databases which have been used to define the models when analyzing the burn process where $T=\frac{\theta}{r}+T_0$. In the tumor, and according to the results, the temperature satisfies the interval $55^0C\leq T$, which has the activation energy parameter $E_a=2.69\times10^5$ J/mol and $E_a/\eta=35406.7$ K^{-1} [43,44].

Results

To obtain the distribution $\theta(r,t)$ in the physical domain, we will use the method of Riemann-sum approximation. We can invert any function in the Laplace transform domain to the time domain as [15]:

$$Z(t)=\frac{e^{\varepsilon t}}{t}\left[\frac{1}{2}\bar{Z}(\varepsilon)+\mathrm{Re}\sum_{n=1}^{N}(-1)^n\bar{Z}\left(\varepsilon+\frac{in\pi}{t}\right)\right] \tag{27}$$

where $i=\sqrt{-1}$ and *Re* is the real part.

Many experiments have shown that the value of ε satisfies the relation $\varepsilon t\approx 4.7$ offers faster convergence [15].

The value $\left.\frac{\theta(r,t)}{r}\right|_{r=0}$ is undefined, and its limit must be replaced by $\underset{r\to 0}{Lim}\frac{\theta(r,t)}{r}$ and by using L'Hôpital's rule as [41]:

$$\left.\frac{\theta(r,t)}{r}\right|_{r=0} = \underset{r\to 0}{Lim}\frac{\theta(r,t)}{r} = \underset{r\to 0}{Lim}\frac{d\theta(r,t)}{dr} = \left.\frac{d\theta(r,t)}{dr}\right|_{r=0} \tag{28}$$

Where $\frac{d\theta(r,t)}{dr} = r\frac{dT(r,t)}{dr} + \left(T(r,t) - T_0\right)$.

Hence, we get

$$T(r,t)\big|_{r=0} = \left.\frac{d\theta(r,t)}{dr}\right|_{r=0} + T_0 \tag{29}$$

To simulate the thermal response within a small spherical tumor of radius R = 0.003 m, we will use the tumor tissue with material properties, as shown in Table 1[13,22,41].

Table 1: Properties of Tumor tissue Model.

Parameter	Unit	Value	Parameter	Unit	Value
K	$\mathrm{W/m\,K}$	0.778	$\rho_b C_b$	$\mathrm{J/m^3/K}$	4.18×10^6
ρ	$\mathrm{kg/m^3}$	1660	T_0	$^{o}\mathrm{C}$	$^{o}37$
C	$\mathrm{J/kg\,K}$	2540	q_m	$\mathrm{W/m^3}$	29000
w_b	$\mathrm{m^3/s/\,m^3}$	0.0064	R	m	0.003
τ_q, τ_T	s	20, 10	α	V/K	Assumed

The results which are represented in figures will be calculated concerning a wide range of distance $r\left(0 \le r \le R\right)$ and at the time $t = (120,150,210)\,s$, different values of voltage *V(V),* and electrical resistance $R_e = (75,600,1300)\,\Omega$. The value $75\,\Omega$ is

the mean value of the resistance of the myxoid liposarcoma tumor, $600\,\Omega$ is the mean value of the resistance of the liposarcoma tumor, and $1300\,\Omega$ is the mean value of the resistance of the lipoma tumor [13]. In the figures based on the distance of the tumor, the horizontal axis has been taken in reverse order to scale the temperature and the damage from the surface of the tumor $r = R$ up to the center $r = 0$.

Discussion

There are no significant histological differences between the electroporated tumor volume and the remaining regions of the tumor mass. On the other hand, and interestingly, different tumor types show different electrical conduction. So, the resistance values have been considered according to tumor histotype [13].

Figures 2-4 show the absolute temperature of myxoid liposarcoma tumor $\{V = 34V, R_e = 75\ \Omega, t = 120\,s\}$, liposarcoma $\{V = 78V, R_e = 600\ \Omega, t = 150\,s\}$, and lipoma tumor $\{V = 84V, R_e = 1300\ \Omega, t = 210\,s\}$, respectively, with different values of the Seebeck coefficient $\alpha = (0.0, 30, 60)V/K$. We choose the values of voltage and time due to the values of the resistance of the three types of tumors. That figures show that the Seebeck coefficient has significant effects on the absolute temperature of myxoid liposarcoma tumors. At the same time, its impact somehow is limited to liposarcoma tumors and lipoma tumors. Moreover, the absolute temperature of the tumors decreases when the value of the Seebeck coefficient increases. Also, the absolute temperature of the tumors decreases when the value of *r* decreases where the thermoelectrical source is located on the surface of the tumor.

Figure 5 shows the absolute temperature of myxoid liposarcoma tumor with different values of voltage $V = (34, 35, 36)V$ with a wide range of distance $0 \le r(m) \le R(m)$ and at the instant of time $t = 120\,s$ when the Seebeck coefficient is $\alpha = 30\ V/K$.

The absolute temperature of the tumor increases when the value of V increases. The mean values of the absolute temperature for three voltages are $T = (60.13,\ 61.47,\ 62.85)\ ^oC$.

Figure 6 shows the absolute temperature of the liposarcoma tumor with different values of voltage $V = (78, 80, 82)V$ with a wide range of distance $0 \le r(m) \le R(m)$ and an instant of time $t = 150\,s$ when the Seebeck coefficient is $\alpha = 30\ V/K$. The absolute temperature of the tumor increases when the value of V increases. The mean values of the absolute temperature for three voltages are $T = (59.27,\ 60.39,\ 61.53)\ ^oC$.

Figure 7 shows the absolute temperature of lipoma tumors with different values of voltage $V = (84, 86, 88)V$ with a wide range of distance $0 \le r(m) \le R(m)$ and an instant of time $t = 210\,s$ when the Seebeck coefficient is $\alpha = 30\ V/K$. The absolute temperature of the tumor increases when the value of V increases. The mean values of the absolute temperature for three voltages are $T = (57.72,\ 58.68,\ 59.66)\ ^oC$.

Figure 8 shows the absolute temperature of myxoid liposarcoma tumor with different values of time $t = (120, 122, 124)\,s$ with a wide range of distance $0 \le r(m) \le R(m)$ when voltage $V = 34V$ and Seebeck coefficient is $\alpha = 30\ V/K$. The absolute temperature of the tumor increases when the value of t increases. The mean values of the absolute temperature for three voltages are $T = (60.13,\ 60.76,\ 61.40)\ ^oC$.

Figure 9 shows the absolute temperature of liposarcoma tumors with different values of time $t = (150, 154, 156)\,s$ with a wide range of distance $0 \le r(m) \le R(m)$ when voltage $V = 78V$ and Seebeck coefficient is $\alpha = 30\ V/K$. The absolute temperature

of the tumor increases when the value of t increases. The mean values of the absolute temperature for three voltages are $T=\left(59.27,\ 60.23,\ 61.20\right)^{o}C$.

Figure 10 shows the absolute temperature of lipoma tumors with different values of time $t=\left(210,214,218\right)s$ with a wide range of distance $0\le r\left(m\right)\le R\left(m\right)$ when voltage $V=84V$ and Seebeck coefficient is $\alpha=30\ V/K$. The absolute temperature of the tumor increases when the value of t increases. The mean values of the absolute temperature for three voltages are $T=\left(57.72,\ 58.82,\ 59.45\right)^{o}C$.

The most important part of this study and the main objective is to determine the quantity of the irreversible damage of the tumors. Figures 11-16 represent the thermal damage of myxoid liposarcoma tumor, liposarcoma tumor, and lipoma tumor with different values of voltage and time, respectively. For three types of tumors, increasing both voltage and time leads to increasing the thermal damage quantity of the tumors. A horizontal line through the thermal damage value $\omega=1.0$ has been added to separate between the reversible and irreversible thermal damage area. The intersection points of this line with the curves give a distance r_o such that $r\ge r_0$ it provides the length of the irreversible thermal damage while $r<r_0$ gives the length of the reversible thermal damage. The formula can calculate the ratio of the volume of the irreversible thermal damage:

$$Vol_{damage}\left(\%\right)=\left(1-\frac{r_o^3}{R^3}\right)\times100 \tag{30}$$

Figures 17-19 represent the thermal damage distribution of myxoid liposarcoma tumor, liposarcoma tumor, and lipoma tumor, respectively, with different values of Seebeck coefficient, different values of voltage, and different values time to study the effect of all that parameters on the quantity of thermal damage on the three types of tumors. The Seebeck coefficient has a

significant impact on the amount of thermal damage for all three types of tumors.

Thus, tables 2-7 contain the ratios of the volume of the irreversible thermal damage quantities, which have been calculated with respect to the distance r_o and different values of the voltage *V* and the time *t*, respectively. Those tables contain the required voltage and time to get significant ratios of the volume of the irreversible thermal damage for the three types of tumors.

Thus, tables 8-10 contain the ratios of the volume of the irreversible thermal damage quantities, which have been calculated with respect to the distance r_o and different values of the Seebeck coefficient α. Those tables inform us about the effect of the Thomson effect on the ratios of the volume of the irreversible thermal damage for the three types of tumors. Considering the Thomson effect leads to a smaller quantity of irreversible thermal damage to the tumors more than the case that does not include this effect.

Table 2: The irreversible thermal damage of myxoid liposarcoma tumor at $t = 120\,s$.

Voltage *V*	Distance r_0	Vol_{damage}
34 v	0.00222 m	59.48 %
35 v	0.00114 m	94.51 %
36 v	$r_0 > R$	100 %

Table 3: The irreversible thermal damage of liposarcoma tumor at $t = 150\,s$.

Voltage *V*	Distance r_0	Vol_{damage}
78 v	0.00234 m	52.54 %
80 v	0.00138 m	90.27 %
82 v	$r_0 > R$	100 %

Table 4: The irreversible thermal damage of lipoma tumor at $t = 210\,s$.

Voltage V	Distance r_0	Vol_{damage}
84 v	0.00279 m	19.56 %
86 v	0.00195 m	72.54 %
88 v	$r_0 > R$	100 %

Table 5: The irreversible thermal damage of myxoid liposarcoma tumor at and voltage $V = 34V$.

Time t	Distance r_0	Vol_{damage}
120 s	0.00222 m	59.48 %
122 s	0.00174 m	80.49 %
124 s	0.00102 m	96.07 %

Table 6: The irreversible thermal damage of liposarcoma tumor at a voltage $V = 78V$.

Time t	Distance r_0	Vol_{damage}
150 s	0.00234 m	52.54 %
154 s	0.00144 m	88.94 %
156 s	$r_0 > R$	100 %

Table 7: The irreversible thermal damage of lipoma tumor at a voltage $V = 84V$.

Time t	Distance r_0	Vol_{damage}
210 s	0.00249 m	19.56 %
214 s	0.00147 m	88.24 %
218 s	0.00039 m	99.78 %

Table 8: The irreversible thermal damage of myxoid liposarcoma tumor with various Seebeck coefficients and at voltage $V = 34V$ and time $t = 120\,s$.

Seebeck α	Distance r_0	Vol_{damage}
0.00 V/K	0.00207 m	67.15 %
30.0 V/K	0.00222 m	59.48 %
60.0 V/K	0.00237 m	50.70 %

Table 9: The irreversible thermal damage of liposarcoma tumor with various Seebeck coefficients and at voltage $V = 78V$ and time $t = 150\,s$.

Seebeck α	Distance r_0	Vol_{damage}
0.00 V/K	0.00228 m	56.10 %
30.0 V/K	0.00234 m	52.54 %
60.0 V/K	0.00240 m	48.80 %

Table 10: The irreversible thermal damage of lipoma tumor with various Seebeck coefficients and at voltage $V = 84V$ and time $t = 210\,s$.

Seebeck α	Distance r_0	Vol_{damage}
0.00 V/K	0.00276 m	23.23 %
30.0 V/K	0.00279 m	19.56 %
60.0 V/K	0.00285 m	14.26 %

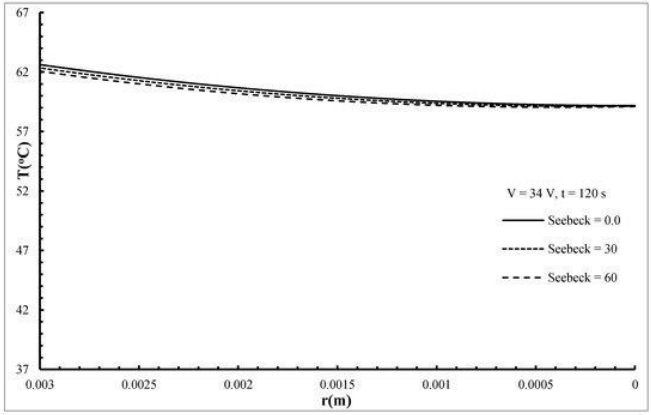

Figure 2: The absolute temperature distribution of myxoid liposarcoma tumor with various values of Seebeck coefficient when $V = 34V, R_e = 75\ \Omega, t = 120\,s$.

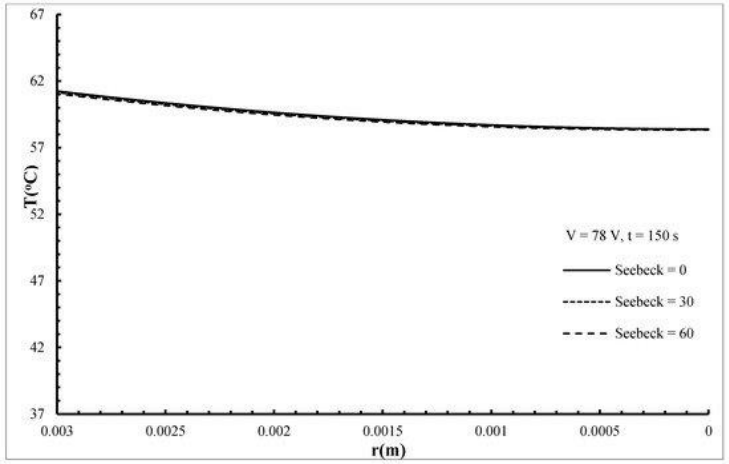

Figure 3: The absolute temperature distribution of liposarcoma tumor with various values of Seebeck coefficient when $V = 78V, R_e = 600\ \Omega, t = 150\,s$.

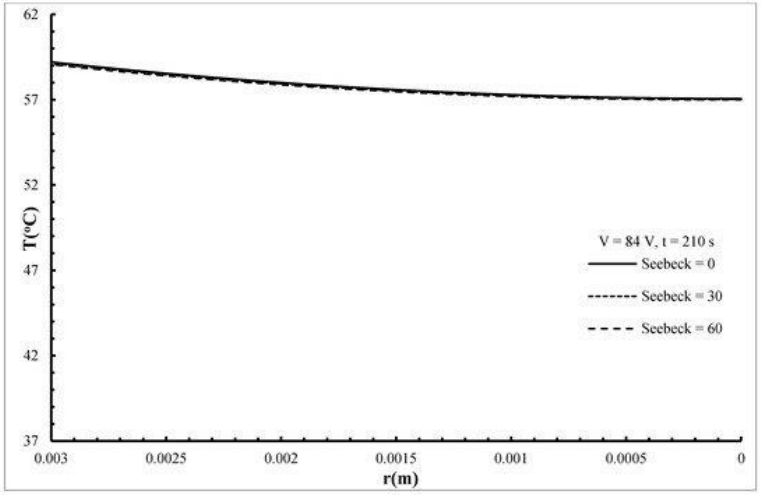

Figure 4: The absolute temperature distribution of lipoma tumor with various values of Seebeck coefficient when $V = 84V, R_e = 1300\ \Omega, t = 210\,s$.

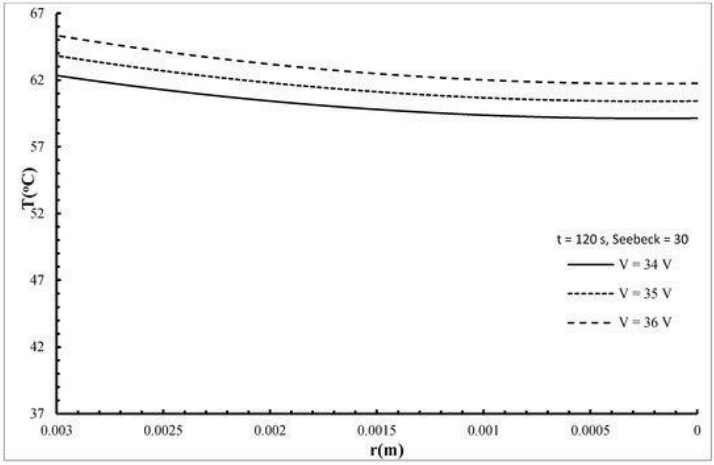

Figure 5: The absolute temperature distribution of myxoid liposarcoma tumor with various values of voltage when $R_e = 75\ \Omega$.

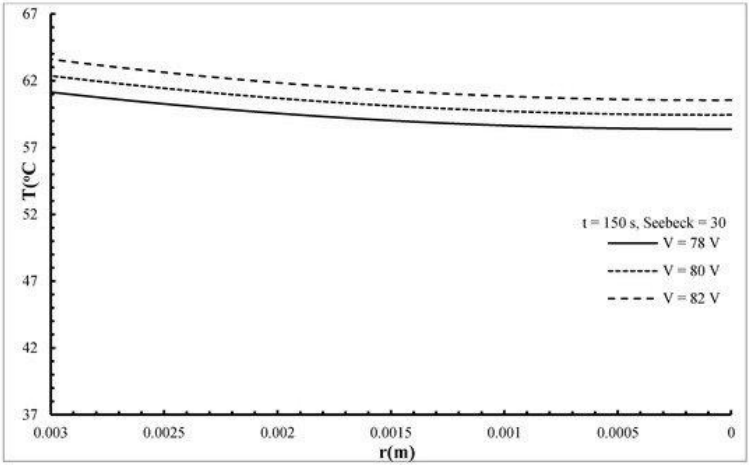

Figure 6: The absolute temperature distribution of liposarcoma tumor with various values of voltage when $R_e = 600\Omega$.

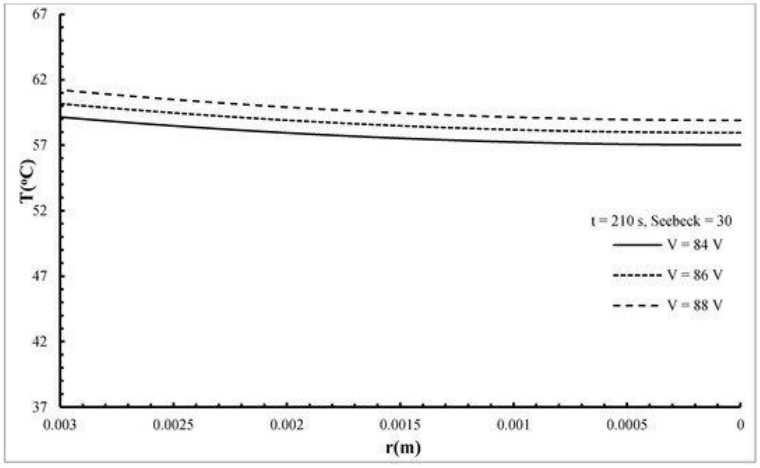

Figure 7: The absolute temperature distribution of lipoma tumor with various values of voltage when $R_e = 1300\Omega$.

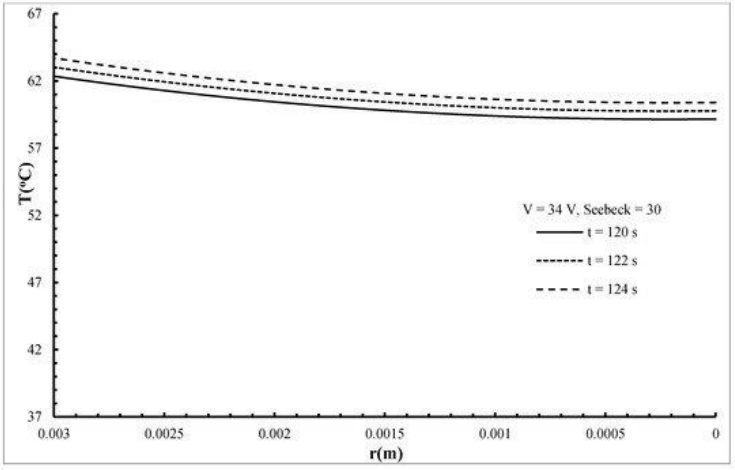

Figure 8: The absolute temperature distribution of myxoid liposarcoma tumor with various values of time $R_e = 75\Omega$.

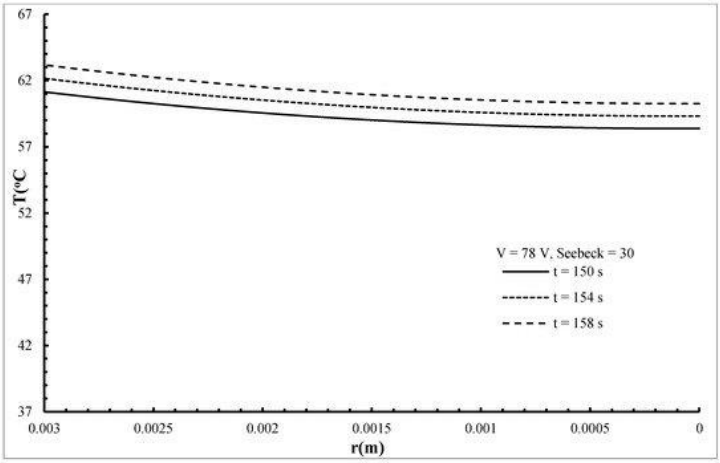

Figure 9: The absolute temperature distribution of liposarcoma tumor with various values of time when $R_e = 600\Omega$.

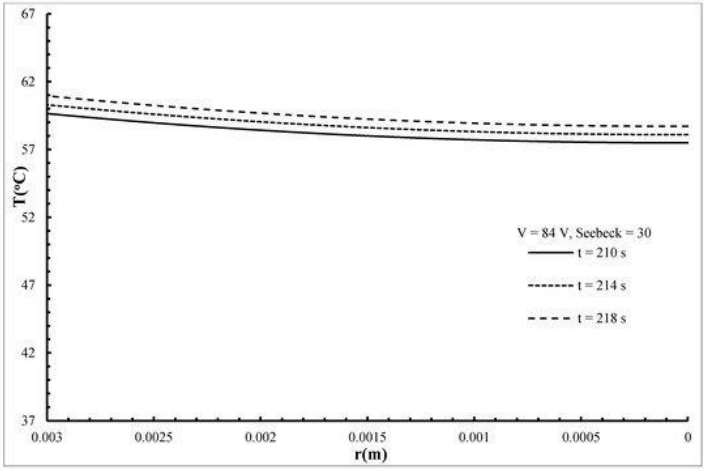

Figure 10: The absolute temperature distribution of lipoma tumor with various values of time when $R_e = 1300\Omega$.

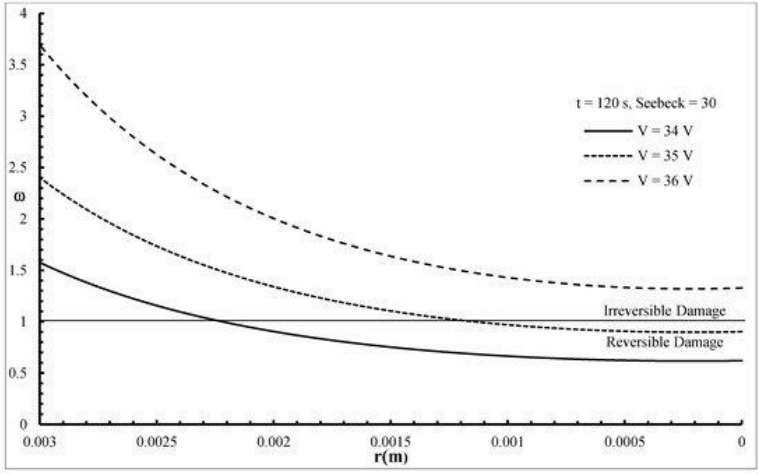

Figure 11: The thermal damage distribution of myxoid liposarcoma tumor with various values of voltage when $R_e = 75\Omega$.

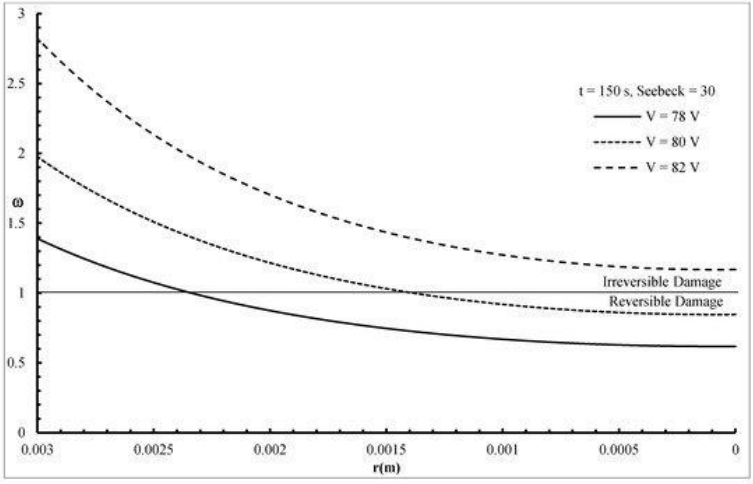

Figure 12: The thermal damage distribution of liposarcoma tumor with various values of voltage when $R_e = 600\Omega$.

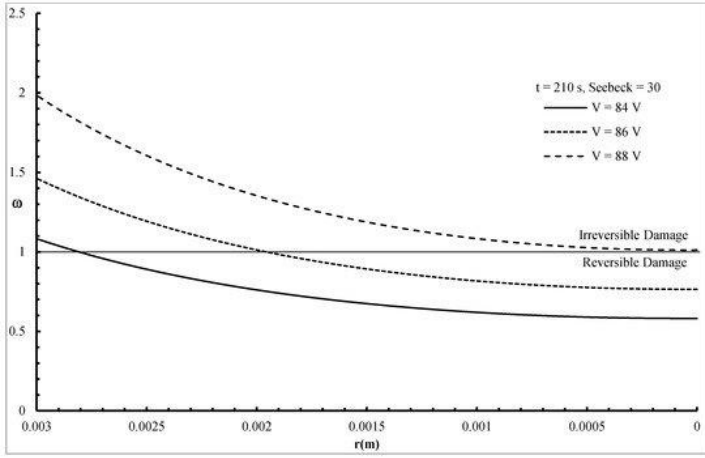

Figure 13: The thermal damage distribution of lipoma tumor with various values of voltage when $R_e = 1300\Omega$.

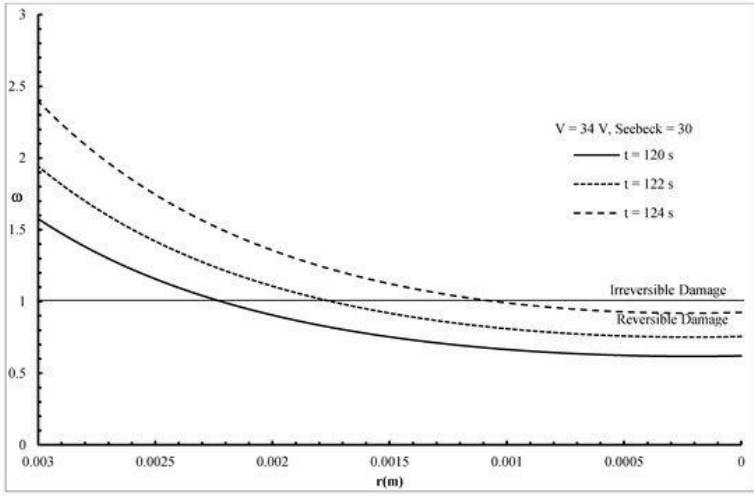

Figure 14: The thermal damage distribution of myxoid liposarcoma tumor with various values of time when $R_e = 75\Omega$.

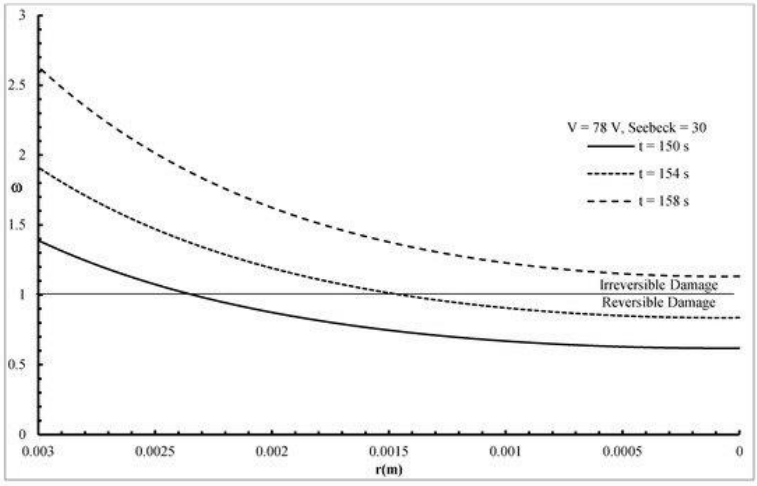

Figure 15: The thermal damage distribution of liposarcoma tumor with various values of time when $R_e = 600\Omega$.

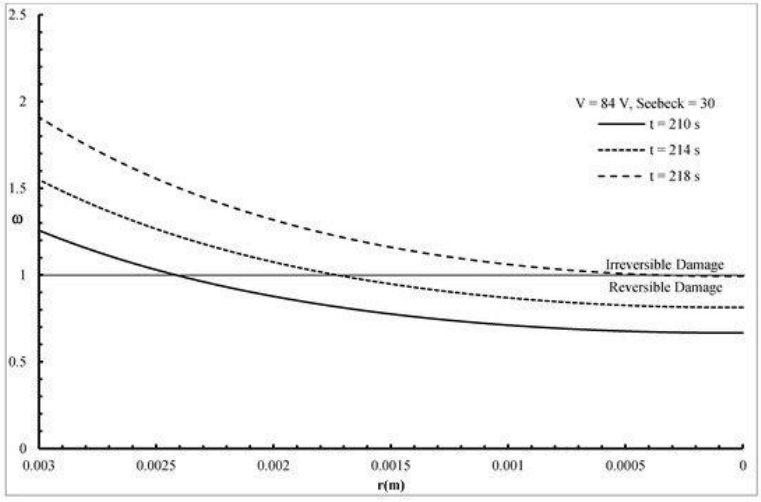

Figure 16: The thermal damage distribution of lipoma tumor with various values of time when $R_e = 1300\Omega$.

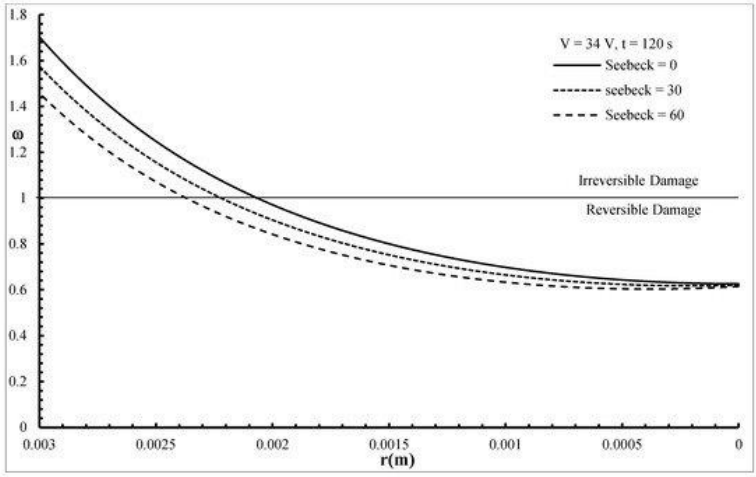

Figure 17: The thermal damage distribution of myxoid liposarcoma tumor with various values of the Seebeck coefficient when $R_e = 75\Omega$.

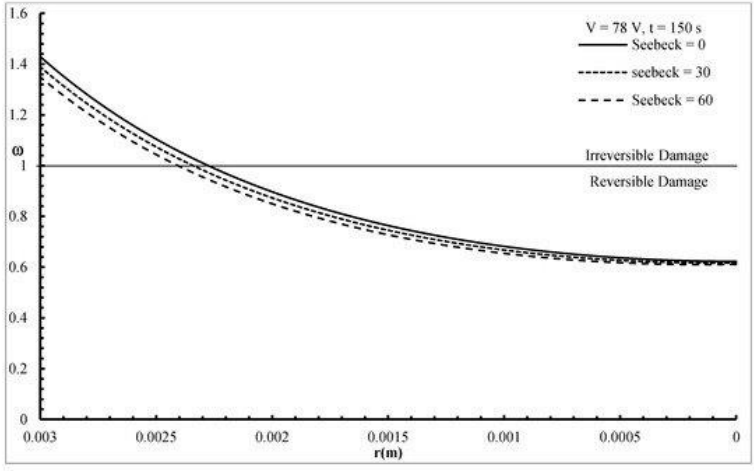

Figure 18: The thermal damage distribution of liposarcoma tumor with various values of the Seebeck coefficient when $R_e = 600\Omega$.

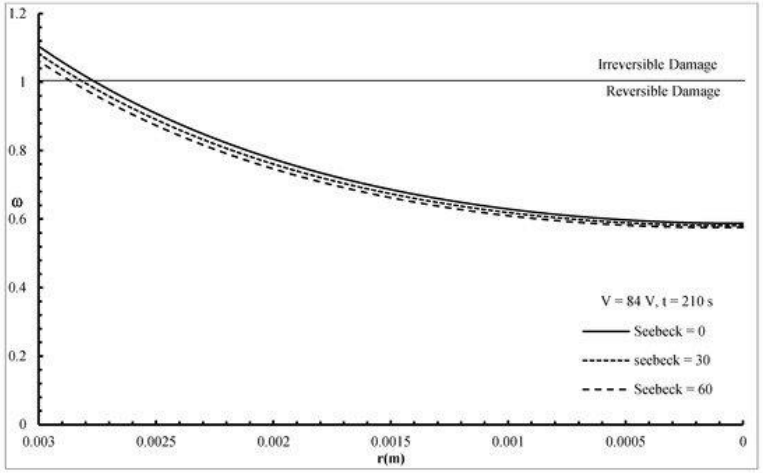

Figure 19: The thermal damage distribution of lipoma tumor with various values of the Seebeck coefficient when $R_e = 1300\Omega$.

Conclusions

In this work, governing partial differential equation of tumor tissue in concentric spherical space based on thermal lagging effect and Thomson effect is solved in the Laplace transform domain. The surface of the tumor tissue is subjected to an electric voltage. The results represent the effects of the different values of voltages, Thomson effect, and times on myxoid liposarcoma tumor, liposarcoma tumor, and lipoma tumor. We focused our attention on the difference value of electrical resistance of the three types of tumors which have been used.

The time and the applied voltages on the surface of the tumors have significant effects on the absolute temperature and the quantity of the irreversible thermal damage to the three types of tumors used.

The Thomson effect has a significant impact on the absolute temperature and the quantity of the irreversible thermal damage of the three types of tumors used.

Applying electrical potential within the electrochemotherapy for some seconds maybe is enough to get the irreversible damage of the myxoid liposarcoma tumor, liposarcoma tumor, and lipoma tumor, which makes electrochemotherapy is a successful treatment.

This research offers a new and potentially effective method in the treatment of cancer that has the characteristic sin of the specific place and its known electrical qualities within the patient's body.

Therefore, we direct the clinical trial operators to try these results on a sample of patients, and we emphasize that these trials are likely to be very successful if the accuracy and study are done.

References

1. Mir LM, Orlowski S. Mechanisms of electrochemotherapy. Advanced drug delivery reviews. 1999; 35: 107-118.
2. Marty M, Sersa G, Garbay JR, Gehl J, Collins CG, et al. Electrochemotherapy–An easy, highly effective and safe treatment of cutaneous and subcutaneous metastases: Results of ESOPE (European Standard Operating Procedures of Electrochemotherapy) study. European Journal of Cancer Supplements. 2006; 4: 3-13.
3. Miklavčič D, Pavšelj N, Hart FX. Electric properties of tissues. Wiley encyclopedia of biomedical engineering. 2006.
4. Nuccitelli R. Application of pulsed electric fields to cancer therapy. Bioelectricity. 2019; 1: 30-34.
5. Gabriel S, Lau R, Gabriel C. The dielectric properties of biological tissues: II. Measurements in the frequency range 10 Hz to 20 GHz. Physics in medicine & biology. 1996; 41: 2251-2269.
6. Čorović S, Županič A, Kranjc S, Al Sakere B, Leroy-Willig A, et al. The influence of skeletal muscle anisotropy on electroporation: in vivo study and numerical modeling. Medical & biological engineering & computing. 2010; 48: 637-648.

7. Davalos RV, Rubinsky B, Otten DM. A feasibility study for electrical impedance tomography as a means to monitor tissue electroporation for molecular medicine. IEEE Transactions on Biomedical Engineering. 2002; 49: 400-403.
8. Ivorra A, Al-Sakere B, Rubinsky B, Mir LM. In vivo electrical conductivity measurements during and after tumor electroporation: conductivity changes reflect the treatment outcome. Physics in Medicine & Biology. 2009; 54: 5949-5963.
9. Laufer S, Ivorra A, Reuter VE, Rubinsky B, Solomon SB. Electrical impedance characterization of normal and cancerous human hepatic tissue. Physiological measurement. 2010; 31: 995-1009.
10. Pavšelj N, Préat V, Miklavčič D. A numerical model of skin electropermeabilization based on in vivo experiments. Annals of biomedical engineering. 2007; 35: 2138-2144.
11. Pliquett U, Langer R, Weaver JC. Changes in the passive electrical properties of human stratum corneum due to electroporation. Biochimica et Biophysica Acta (BBA)-Biomembranes. 1995; 1239: 111-121.
12. Tsai B, Xue H, Birgersson E, Ollmar S, Birgersson U. Dielectrical properties of living epidermis and dermis in the frequency range from 1 kHz to 1 MHz. Journal of Electrical Bioimpedance. 2019; 10: 14-23.
13. Campana LG, Dughiero F, Forzan M, Rastrelli M, Sieni E, et al. Electrical resistance of tumor tissue during electroporation: an ex-vivo study on human lipomatous tumors. In Proceedings of 6th European Conference of the International Federation for Medical and Biological Engineering. 2020; 569-572.
14. Tzou DY. The generalized lagging response in small-scale and high-rate heating. International Journal of Heat and Mass Transfer. 1995; 38: 3231-3240.
15. Tzou DY. Macro-to microscale heat transfer: the lagging behavior. New Jersey: John Wiley & Sons. 2014.
16. Antaki PJ. Solution for non-Fourier dual phase lag heat conduction in a semiinfinite slab with surface heat flux. International Journal of Heat and Mass Transfer. 1998; 41: 2253-2258.

17. Tang D, Araki N. Non-fourier heat condution behavior in finite mediums under pulse surface heating. Materials Science and Engineering: A 2000; 292: 173-178.
18. Al-Nimr M, Al-Huniti NS. Transient thermal stresses in a thin elastic plate due to a rapid dual-phase-lag heating. Journal of thermal stresses. 2000; 23: 731-746.
19. Nassar WDR. A finite difference method for solving 3-D heat transport equations in a double-layered thin film with microscale thickness and nonlinear interfacial conditions. Numerical Heat Transfer: Part A: Applications. 2001; 39: 21-33.
20. Dai W, Shen L, Zhu T. A stable three-level finite-difference scheme for solving a three-dimensional dual-phase-lagging heat transport equation in spherical coordinates. Numerical Heat Transfer. Part B: Fundamentals. 2004; 46: 121-139.
21. Liu KC, Cheng PJ. Numerical analysis for dual-phase-lag heat conduction in layered films. Numerical Heat Transfer. Part A: Applications. 2006; 49: 589-606.
22. Liu KC, Chen HT. Analysis for the dual-phase-lag bio-heat transfer during magnetic hyperthermia treatment. International Journal of Heat and Mass Transfer. 2009; 52: 1185-1192.
23. Antaki PJ. New interpretation of non-Fourier heat conduction in processed meat. Journal of Heat Transfer. 2005; 127: 189-193.
24. Mitra K, Kumar S, Vedevarz A, Moallemi M. Experimental evidence of hyperbolic heat conduction in processed meat. Journal of Heat Transfer. 1995; 117: 568-573.
25. Liu KC, Chen HT. Investigation for the dual phase lag behavior of bio-heat transfer. International Journal of Thermal Sciences. 2010; 49: 1138-1146.
26. Liu KC, Lin CT. Solution of an inverse heat conduction problem in a bi-layered spherical tissue. Numerical Heat Transfer, Part A: Applications. 2010; 58: 802-818.
27. Tzou DY, Dai W. Thermal lagging in multi-carrier systems. International Journal of Heat and Mass Transfer. 2009; 52: 1206-1213.
28. Tzou D, Guo ZY. Nonlocal behavior in thermal lagging. International Journal of Thermal Sciences. 2010; 49: 1133-1137.

29. Tzou D. Lagging behavior in biological systems. Journal of Heat Transfer. 2012; 134: 051006.
30. Martirosyan NL, Rutter EM, Ramey WL, Kostelich EJ, Kuang Y, et al. Mathematically modeling the biological properties of gliomas: a review. Mathematical Biosciences & Engineering. 2015; 12: 879-905.
31. Calzado EM, Rodríguez JLG, Cabrales LEB, García FM, Castaneda ARS, et al. Simulations of the electrostatic field, temperature, and tissue damage generated by multiple electrodes for electrochemical treatment. Applied Mathematical Modelling. 2019; 76: 699-716.
32. Soba A, Suárez C, González MM, Cabrales LEB, Pupo AEB, et al. Integrated analysis of the potential, electric field, temperature, pH and tissue damage generated by different electrode arrays in a tumor under electrochemical treatment. Mathematics and Computers in Simulation. 2018; 146: 160-176.
33. Aguilera AR, Cabrales LEB, Ciria HMC, Pérez YS, González FG, et al. Electric current density distribution in planar solid tumor and its surrounding healthy tissue generated by an electrode elliptic array used in electrotherapy. Mathematics and Computers in Simulation. 2010; 80: 1886-1902.
34. Luo C, Xu S, Dai G, Xiao Z, Chen L, et al. Tumor treating fields for high-grade gliomas. Biomedicine & Pharmacotherapy. 2020; 127: 110193.
35. Lashkevych I, Velázquez J, Titov OY, Gurevich YG. Special Important Aspects of the Thomson Effect. Journal of Electronic Materials. 2018; 47: 3189-3192.
36. Chen J, Yan Z, Wu L. The influence of Thomson effect on the maximum power output and maximum efficiency of a thermoelectric generator. Journal of applied physics. 1996; 79: 8823-8828.
37. Karimipour A, D'Orazio A, Goodarzi M. Develop the lattice Boltzmann method to simulate the slip velocity and temperature domain of buoyancy forces of FMWCNT nanoparticles in water through a micro flow imposed to the specified heat flux. Physica A: Statistical Mechanics and Its Applications. 2018; 509: 729-745.

38. Pordanjani AH, Aghakhani S, Karimipour A, Afrand M, Goodarzi M. Investigation of free convection heat transfer and entropy generation of nanofluid flow inside a cavity affected by magnetic field and thermal radiation. Journal of Thermal Analysis and Calorimetry. 2019; 137: 997-1019.
39. Goodarzi H, Akbari OA, Sarafraz MM, Karchegani MM, Safaei MR, et al. Numerical simulation of natural convection heat transfer of nanofluid with Cu, MWCNT, and Al2O3 nanoparticles in a cavity with different aspect ratios. Journal of Thermal Science and Engineering Applications. 2019; 25: 11.
40. Zhou J, Chen J, Zhang Y. Dual-phase lag effects on thermal damage to biological tissues caused by laser irradiation. Computers in Biology and Medicine. 2009; 39: 286-293.
41. Liu KC. Nonlinear behavior of thermal lagging in concentric living tissues with Gaussian distribution source. International Journal of Heat and Mass Transfer. 2011; 54: 2829-2836.
42. El-Bary AA, Youssef HM, Omar M, Ramadan KT. Influence of thermal wave emitted by the cellular devices on the human head. Microsystem Technologies. 2019; 25: 413-422.
43. Moritz AR, Henriques Jr F. Studies of thermal injury: II. The relative importance of time and surface temperature in the causation of cutaneous burns. The American journal of pathology. 1947; 23: 695-720.
44. Henriques Jr F, Moritz A. Studies of thermal injury: I. The conduction of heat to and through skin and the temperatures attained therein. A theoretical and an experimental investigation. The American journal of pathology. 1947; 23: 530-549.
45. Majchrzak E, Jasiński M. Sensitivity analysis of burns integrals. Computer Assisted Mechanics and Engineering Sciences. 2004; 11: 125-136.
46. Xu F, Lu T. Introduction to skin biothermomechanics and thermal pain. Berlin: Springer. 2011; 7.